Analytic calculation of two-loop QCD corrections to $b \to s\ell^+\ell^-$ in the high q^2 region

C. Greub,* V. Pilipp,† and C. Schüpbach‡

Center for Research and Education in Fundamental Physics,

Institute for Theoretical Physics,

University of Bern

Sidlerstrasse 5, CH-3012 Bern

arXiv:0810.4077v3 [hep-ph] 9 Dec 2008

Abstract

We present our results for the NNLL virtual corrections to the matrix elements of the operators O_1 and O_2 for the inclusive process $b \to s\ell^+\ell^-$ in the kinematical region $q^2 > 4m_c^2$, where q^2 is the invariant mass squared of the lepton-pair. This is the first analytic two-loop calculation of these matrix elements in the high q^2 region. We give the matrix elements as an expansion in m_c/m_b and keep the full analytic dependence on q^2. Making extensive use of differential equation techniques, we fully automatize the expanding of the Feynman integrals in m_c/m_b. In coincidence with an earlier work where the master integrals were obtained numerically [1], we find that in the high q^2 region the α_s corrections to the matrix elements $\langle s\ell^+\ell^-|O_{1,2}|b\rangle$ calculated in the present paper lead to a decrease of the perturbative part of the q^2-spectrum by $10\% - 15\%$ relative to the NNLL result in which these contributions are put to zero and reduce the renormalization scale uncertainty to $\sim 2\%$.

*Electronic address: christoph.greub@itp.unibe.ch

†Electronic address: volker.pilipp@itp.unibe.ch

‡Electronic address: christof.schuepbach@itp.unibe.ch

I. INTRODUCTION

Flavor-changing neutral currents play an important role in the indirect search for new physics. For inclusive decays there exists the framework of operator-product expansion, which makes theoretically clean predictions possible. Of special interest in this context is the decay mode $B \to X_s \ell^+ \ell^-$. In the regions where the lepton invariant mass squared q^2 is far away from the $c\bar{c}$-resonances, the dilepton invariant mass spectrum and the forward-backward asymmetry can be precisely predicted.

The status of the calculation of these observables is the following: The leading logarithmic (LL) and the next-to-leading logarithmic (NLL) QCD contributions were calculated in [2, 3, 4]. Next-to-next-to-leading logarithmic (NNLL) corrections to the Wilson coefficients at the matching scale $\mu \sim m_W$, which required to perform two-loop matching calculations of the full standard model (SM) theory onto the effective theory, have been worked out in [5, 6, 7, 8]. The anomalous dimensions matrices needed to obtain the Wilson coefficients at the low scale $\mu \sim m_b$ (requiring up to three-loop calculations for certain entries) were obtained in [5, 9, 10, 11, 12]. NNLL QCD corrections at the level of the matrix elements of the operators involved were calculated for the dilepton invariant mass spectrum and for the forward-backward asymmetry in [1, 13, 14, 15, 16, 17]. Power corrections of the order $1/m_b^2$, $1/m_c^2$ and $1/m_b^3$ have been worked out in [18, 19, 20, 21, 22, 23, 24]. Finally, in [25, 26, 27] certain classes of logarithmically enhanced electromagnetic corrections were taken into account.

So far, *analytic results* for the NNLL QCD corrections to the matrix elements associated with the operators O_1 and O_2 are only available in the region of low q^2. The corresponding results were obtained as a double-expansion in m_c/m_b and q^2/m_b^2 [13, 14, 15]. The present paper deals with the NNLL QCD corrections in the high q^2 region, i.e. $q^2 > 4m_c^2$. In particular we evaluate *virtual* QCD corrections to the matrix elements of the operators O_1 and O_2 at order α_s. In contrast to [1], where the relevant master integrals were calculated numerically, we present these matrix elements as analytic functions of m_c and q^2. The purpose of the present paper is twofold: First, to deliver a non-trivial independent check of the results found in [1] and second, to provide the user with analytic formulas in which the parameters (m_c/m_b and μ/m_b) and q^2 can easily be changed.

To get these analytic results, we perform an expansion in m_c/m_b and keep the full analytic

dependence on q^2. We expand the two-loop Feynman integrals by combining method of regions [28, 29, 30, 31] and differential equation techniques [32, 33, 34, 35]. We end up with an expansion of $\langle s\ell^+\ell^-|O_{1,2}|b\rangle$ up to the 20th power in m_c/m_b. As the resulting expressions for these matrix elements are rather lengthy, we are not able to print them in the paper. We provide Mathematica and c++ code of our results in the source files of the present paper at arXiv.

The well-known breakdown of the Λ/m_b expansion at the endpoint $q^2 = m_B^2$ seems to question the relevance of the perturbative contributions in the high q^2-region calculated in this paper. However, as it was shown in [36] and [37] (illustated there for the analogous lepton invariant mass spectrum in the inclusive semileptonic decay $B \to X_u\ell\nu$) that the integrated high q^2-spectrum allows for a modified version of the heavy-quark expansion (the so-called hybrid expansion), our present work is well-motivated.

The paper is organized as follows. Sections II and III are dedicated to the technical details of the calculation. We give all necessary definitions in Section II. In Section III we explain the evaluation of the Feynman integrals in detail. In Section IV we investigate the (numerical) stability of the expansion in m_c/m_b, concluding that retaining terms up to the 20th power in m_c/m_b leads to precise results. In this Section we also discuss the numerical impact of our calculation on the dilepton invariant mass spectrum. In coincidence with [1] we find that in the high q^2 region the order α_s corrections to the matrix elements $\langle s\ell^+\ell^-|O_{1,2}|b\rangle$ calculated in the present paper lead to a decrease of the perturbative part of the q^2-spectrum by $10\% - 15\%$ relative to the NNLL result in which these corrections are put to zero and reduce the renormalization scale uncertainty to $\sim 2\%$.

II. DEFINITIONS

As in the previous paper [14] we write the effective Hamiltonian that contributes to $B \to X_s\ell^+\ell^-$ in the form

$$\mathcal{H}_{\text{eff}} = -\frac{4G_F}{\sqrt{2}} V_{ts}^* V_{tb} \sum_{i=1}^{10} C_i(\mu) O_i(\mu), \tag{1}$$

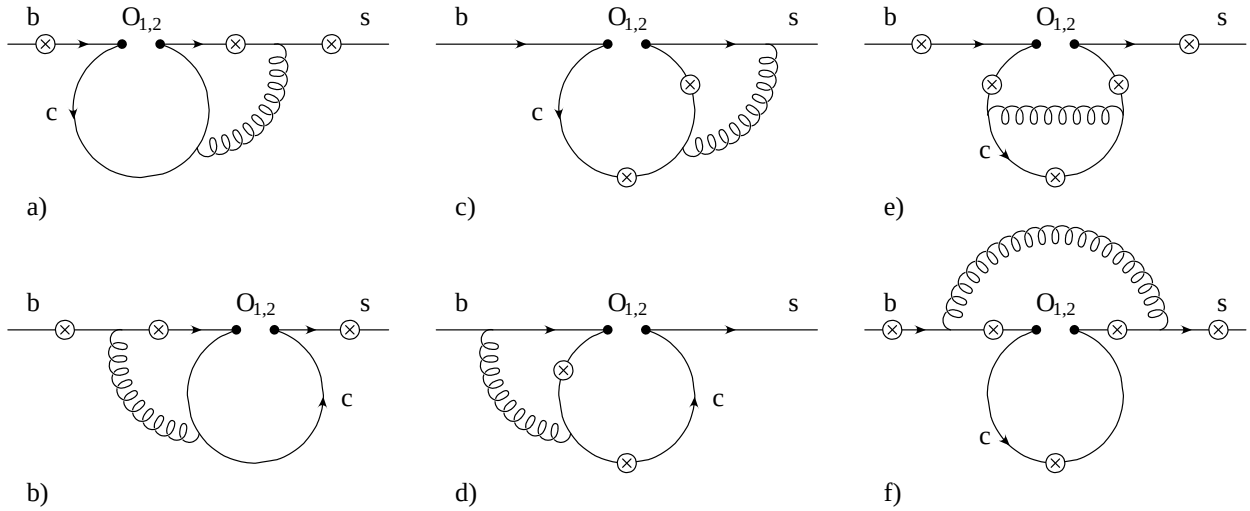

FIG. 1: Diagrams that have to be taken into account at order α_s. The circle-crosses denote the possible locations where the virtual photon is emitted (see text).

where we have neglected the small CKM combination $V_{us}^* V_{ub}$. The operator basis is defined as

$$
\begin{aligned}
O_1 &= (\bar{s}_L\gamma_\mu T^a c_L)(\bar{c}_L\gamma^\mu T^a b_L)\,, & O_2 &= (\bar{s}_L\gamma_\mu c_L)(\bar{c}_L\gamma^\mu b_L)\,,\\
O_3 &= (\bar{s}_L\gamma_\mu b_L)\textstyle\sum_q(\bar{q}\gamma^\mu q)\,, & O_4 &= (\bar{s}_L\gamma_\mu T^a b_L)\textstyle\sum_q(\bar{q}\gamma^\mu T^a q)\,,\\
O_5 &= (\bar{s}_L\gamma_\mu\gamma_\nu\gamma_\rho b_L)\textstyle\sum_q(\bar{q}\gamma^\mu\gamma^\nu\gamma^\rho q)\,, & O_6 &= (\bar{s}_L\gamma_\mu\gamma_\nu\gamma_\rho T^a b_L)\textstyle\sum_q(\bar{q}\gamma^\mu\gamma^\nu\gamma^\rho T^a q)\,,\\
O_7 &= \tfrac{e}{g_s^2}m_b(\bar{s}_L\sigma^{\mu\nu}b_R)F_{\mu\nu}\,, & O_8 &= \tfrac{1}{g_s}m_b(\bar{s}_L\sigma^{\mu\nu}T^a b_R)G^a_{\mu\nu}\,,\\
O_9 &= \tfrac{e^2}{g_s^2}(\bar{s}_L\gamma_\mu b_L)\textstyle\sum_l(\bar{l}\gamma^\mu l)\,, & O_{10} &= \tfrac{e^2}{g_s^2}(\bar{s}_L\gamma_\mu b_L)\textstyle\sum_l(\bar{l}\gamma^\mu\gamma_5 l)\,,
\end{aligned}
\tag{2}
$$

where the subscripts L and R refer to left- and right- handed components of the fermion fields. The ingredients to obtain the Wilson coefficients C_i at the scale μ of order m_b can be found e.g. in [5, 8, 10].

In the present publication we calculate the virtual α_s-corrections to the matrix elements of O_1 and O_2 in the large q^2 region. Using equations of motion, we write these α_s-corrections in the form[1]

$$
\langle s\ell^+\ell^-|O_i|b\rangle_{\text{2-loops}} = -\left(\frac{\alpha_s}{4\pi}\right)^2\left[F_i^7\langle O_7\rangle_{\text{tree}} + F_i^9\langle O_9\rangle_{\text{tree}}\right]. \tag{3}
$$

[1] Note that because of the extra factors $1/g_s^2$ in the definition of O_7 and O_9 (3) is indeed of order α_s.

The diagrams that contribute at order α_s to $b \to s\ell^+\ell^-$ are shown in Fig.1. By definition, we include in $F_{1,2}^{(7,9)}$ only the contributions from the diagrams in Fig. 1a-e. As in [14], we absorb the contribution from Fig. 1f into a modified Wilson coefficient C_9. This procedure is convenient, because only the diagram Fig. 1f contains infrared divergences.

The ultraviolet renormalization works analogously to [14]. In particular we use the same evanescent operators. We use on-shell renormalization for the s- and the b-field and renormalize m_c in the pole mass scheme.

The kinematics is defined as follows: We denote the momentum of the incoming b-quark by p and the momentum of the virtual photon by q. The momenta of the external fermions are on-shell such that $p^2 = m_b^2$ and $(p-q)^2 = 0$, because we neglect the strange-quark mass. Furthermore we use the notations

$$\hat{s} = \frac{q^2}{m_b^2} \quad \text{and} \quad z = \frac{m_c^2}{m_b^2}. \tag{4}$$

III. CALCULATION OF THE MASTER INTEGRALS

In the present section we explain for every diagram appearing in Fig. 1 the way we evaluated the master integrals that are specific to it. In Appendix A we list the master integrals that appear in more than one diagram and which are straightforward to calculate.

We use the following notation

$$[dk] = \left(\frac{\mu^2}{4\pi} e^{\gamma_E}\right)^{\epsilon} \frac{d^d k}{(2\pi)^d}, \tag{5}$$

where $d = 4 - 2\epsilon$.

For simplicity we set $m_b = 1$ in the calculation of the master integrals, such that $m_c^2 = z$. The dependence of the master integrals on m_b can be easily restored by dimensional analysis.

A. General remarks about calculation techniques

The Feynman integrals appearing in our calculation have been reduced to a set of master integrals using the following methods: Tensor integrals i.e. integrals containing Lorentz indices have been reduced to scalar integrals via the Passarino-Veltman reduction scheme [38]. Finally these scalar integrals can be further reduced by integration by parts (IBP) identities [39, 40]. In particular we used the algorithm described in [41]. To this end we

used the Maple implementation AIR [42] and a Mathematica implementation developed by us. Since we consider the region $\hat{s} > 4z$, we expanded the master integrals in z and kept the full analytic dependence in $\hat{s}$.

For power expanding Feynman integrals we use a combination of *method of regions* [28, 29, 30, 31] and *differential equation techniques* [32, 33, 34, 35, 43]. We consider a set of Feynman integrals $I_1, \ldots, I_n$ that depend on the expansion parameter z and that are related by a system of differential equations:

$$\frac{d}{dz} I_\alpha = \sum_\beta h_{\alpha\beta} I_\beta + g_\alpha. \tag{6}$$

We obtain (6) by differentiating I_α with respect to z and applying IBP identities, from where we obtain the original set of integrals and further integrals contained in g_α, which are simpler than I_α and have been calculated before. Expanding the objects appearing in (6) in ϵ, z and $\ln z$

$$\begin{aligned} I_\alpha &= \sum_{i,j,k} I_{\alpha,i}^{(j,k)} \epsilon^i z^j (\ln z)^k \\ h_{\alpha\beta} &= \sum_{i,j} h_{\alpha\beta,i}^{(j)} \epsilon^i z^j \\ g_\alpha &= \sum_{i,j,k} g_{\alpha,i}^{(j,k)} \epsilon^i z^j (\ln z)^k, \end{aligned} \tag{7}$$

and inserting (7) into (6) we obtain algebraic equations for the coefficients $I_{\alpha,i}^{(j,k)}$

$$0 = (j+1) I_{\alpha,i}^{(j+1,k)} + (k+1) I_{\alpha,i}^{(j+1,k+1)} - \sum_\beta \sum_{i'} \sum_{j'} h_{\alpha\beta,i'}^{(j')} I_{\beta,i-i'}^{(j-j',k)} - g_{\alpha,i}^{(j,k)}. \tag{8}$$

By means of (8) we can reduce higher powers in z of I_α to lower powers. In practice this means that we need the leading power and sometimes also the next-to-leading power of I_α as initial condition for (8). We have calculated these initial conditions by method of regions. Every region except the hard region leads to logarithms in z. As we obtain the logarithms occurring at leading power both from method of regions and from the recurrence relation (8), differential equations provide a non trivial check for method of regions, i.e. we can make sure not to have forgotten or counted twice any region.

In (7) we did not specify which values the summation index j takes. Indeed we will have to deal with integrals that come with half-integer values of j i.e. they have to be expanded in $\sqrt{z}$. On the other hand we have to presume that there exists $k_{\max}$ such that $I_{\alpha,i}^{(j,k)} = 0$ for

all $k > k_{\max}$ in order to solve (8). We use the algorithm that was described in [34] to get the possible values for j and to determine $k_{\max}$. In addition this algorithm allows us to evaluate the coefficients $I_{\alpha,i}^{(j,k)}$ numerically. We used this feature to test the initial conditions.

In the following we will show in detail how to evaluate the master integrals occurring from the diagrams in Fig. 1 by this procedure.

B. Diagrams of Fig. 1a

The topology of Fig. 1a contains in addition to (A2), (A11), (A12) and (A13), which are easy to evaluate, these two master integrals

$$\begin{aligned} I_{a1} &= \int [dk][dl] \frac{1}{(k+p-q)^2(k+p)^2((k+l)^2-z)(l^2-z)} \\ I_{a2} &= \int [dk][dl] \frac{1}{(k+p-q)^2(k+p)^2((k+l)^2-z)(l^2-z)^2} \end{aligned} \tag{9}$$

where we use the notation (5) and assume implicitly that every denominator contains a positive imaginary part $+i0$. We need both integrals in leading power i.e. at z^0. There are three regions that contribute to this power: The hard region $k^\mu, l^\mu \sim 1$, the soft region $k^\mu \sim 1$, and $l^\mu \sim \sqrt{z}$ and the collinear region where both k and l are collinear to $p-q$ (scaling see below). Both integrals get a leading power contribution in the hard region. The hard region corresponds to setting $z=0$ in the integrand. In this limit we can reduce I_{a2} to I_{a1} by IBP identities. I_{a1} at $z=0$ can by evaluated via Feynman parameterization to

$$I_{a1,h} = -\frac{1}{(4\pi)^4} \left(\mu^2 e^{\gamma_E + i\pi}\right)^{2\epsilon} \frac{\Gamma(\epsilon)\Gamma(2\epsilon)\Gamma^3(1-\epsilon)\Gamma(1-2\epsilon)}{\Gamma(1+\epsilon)\Gamma(2-2\epsilon)\Gamma(2-3\epsilon)} \, {}_2\mathrm{F}_1(2\epsilon, 1; 1+\epsilon; 1-\hat{s}), \tag{10}$$

where

$${}_2\mathrm{F}_1(a,b;c;x) = \frac{\Gamma(c)}{\Gamma(b)\Gamma(c-b)} \int_0^1 dt\, t^{b-1}(1-t)^{c-b-1}(1-tx)^{-a} \tag{11}$$

with $\Re c > \Re b > 0$. We used the Mathematica packages described in [44, 45] to obtain the expansion in ϵ of ${}_2\mathrm{F}_1$.

In the soft region $k^\mu \sim 1$, $l^\mu \sim \sqrt{z}$ only I_{a2} gets a leading power contribution:

$$I_{a2,s} = z^{-\epsilon} \int [dk][dl] \frac{1}{(k+p-q)^2(k+p)^2 k^2 (l^2-1)^2}. \tag{12}$$

Using IBP identities, (12) can be reduced to a product of two simple one-loop integrals.

Let us consider the collinear region. We introduce the following light-like vectors n_+ and n_-, which fulfil $n_+^2 = n_-^2 = 0$ and $n_+ \cdot n_- = 1$. We define the decomposition of a Lorentz vector into light-cone coordinates:

$$k^\mu = k^- n_-^\mu + k^+ n_+^\mu + k_\perp^\mu \tag{13}$$

where $k^\pm = k \cdot n_\mp$. We choose n_+ to be collinear to $p-q$ and introduce the following scaling

$$k^+, l^+ \sim 1, \quad k_\perp, l_\perp \sim \sqrt{z} \quad \text{and} \quad k^-, l^- \sim z. \tag{14}$$

As before, only I_{a2} gets a leading power contribution in this region.

$$I_{a2,c} = z^{-2\epsilon} \int [dk][dl] \frac{1}{(k+p-q)^2(2k^+p^- + 1)((k+l)^2 - 1)(l^2-1)^2}. \tag{15}$$

Via Feynman parameterization we evaluate (15), obtaining

$$\frac{-1}{(4\pi)^4} \left(\mu^2 e^{\gamma_E}\right)^{2\epsilon} \frac{\Gamma^2(\epsilon)}{2\Gamma(1-\epsilon)} \, {}_2\mathrm{F}_1(1,1;2-\epsilon;1-\hat{s}). \tag{16}$$

Finally the leading power contributions of the master integrals up to order ϵ^0 read

$$\begin{aligned} I_{a1}^{(0)} &= \frac{1}{(4\pi)^4} \mu^{4\epsilon} \Bigg[-\frac{1}{2\epsilon^2} + \frac{\ln(\hat{s}) - i\pi - \frac{5}{2}}{\epsilon} \\ &\quad - \frac{1}{2}\ln^2(\hat{s}) + (5+2i\pi)\ln(\hat{s}) + \mathrm{Li}_2(1-\hat{s}) + \frac{13\pi^2}{12} - 5i\pi - \frac{19}{2} \Bigg] \\ I_{a2}^{(0)} &= \frac{1}{(4\pi)^4} \Bigg[\frac{1}{2}\ln(\hat{s})\ln^2(z) + (i\pi\ln(\hat{s}) + \mathrm{Li}_2(1-\hat{s}))\ln(z) \\ &\quad - \frac{\pi^2}{2}\ln(\hat{s}) + i\pi\mathrm{Li}_2(1-\hat{s}) - \mathrm{Li}_3(1-\hat{s}) \Bigg]. \end{aligned} \tag{17}$$

We continue with the calculation of the subleading powers of I_{a1} and I_{a2}. By differentiating I_{a1} and I_{a2} with respect to z and applying IBP identities we obtain a coupled system of differential equations of the form (6) with h starting at order ϵ^0 and z^{-1}. More explicitly (8) becomes

$$0 = (j+1) I_{a\alpha,i}^{(j+1,k)} + (k+1) I_{a\alpha,i}^{(j+1,k+1)} - \sum_{\beta=1,2} \sum_{i'=0}^{i+2} \sum_{j'=-1}^{j} h_{\alpha\beta,i'}^{(j')} I_{a\beta,i-i'}^{(j-j',k)} - g_{\alpha,i}^{(j,k)}. \tag{18}$$

From (18) together with (17) we obtain the subleading powers in z of I_{a1} and I_{a2}. We also obtain the coefficient of the $z^0 \ln z$-term of I_{a2}, which we already calculated in (17). This means that the differential equations provide a non-trivial check for method of regions, which was used for the leading power calculation.

C. Diagrams of Fig. 1b

The topology Fig. 1b comes with the master integrals

$$\begin{aligned}
I_{b1} &= \int [dk][dl] \frac{1}{((k+p)^2-1)((k+p-q)^2-1)(l^2-z)((k+l)^2-z)} \\
I_{b2} &= \int [dk][dl] \frac{1}{((k+p)^2-1)((k+p-q)^2-1)(l^2-z)^2((k+l)^2-z)} \\
I_{b3} &= \int [dk][dl] \frac{1}{((k+p)^2-1)((k+p-q)^2-1)^2(l^2-z)((k+l)^2-z)}.
\end{aligned} \tag{19}$$

We need these integrals in leading power. Besides the hard region, where all of these integrals get a leading power contribution, I_{b2} also gets contributions from two further regions. In the soft region defined by $k^\mu \sim 1$ and $l^\mu \sim \sqrt{z}$ I_{b2} becomes

$$I_{b2,s} = z^{-\epsilon} \int [dk][dl] \frac{1}{((k+p)^2-1)((k+p-q)^2-1)(l^2-1)^2 k^2}, \tag{20}$$

which is a product of (A8) and a trivial tadpole integral. In the collinear region defined by $k^\mu \sim 1, l^+ \sim 1$, $l_\perp \sim \sqrt{z}$ and $l^- \sim z$, I_{b2} takes the form

$$I_{b2,c} = z^{-\epsilon} \int [dk][dl] \frac{1}{((k+p)^2-1)((k+p-q)^2-1)(l^2-1)^2(k^2+2l^+k^-)}. \tag{21}$$

However, the collinear region has an overlap with the soft region, where (21) reduces to (20). On the other hand (21) is indeed equal to (20) which can be seen by the following argument: Consider the integration $[dl]$. The integrand depends besides on terms constant in l^μ only on l^2 and $l^+ = l \cdot n_-$. So n_-^μ is the only Lorentz vector that multiplies l^μ. Because of Lorentz invariance the integral can only depend on n_- through $n_-^2 = 0$. So we can set n_- to zero such that (21) reduces to (20). This is to say the collinear region has already been taken into account by the soft region. To avoid double counting we have to skip the contribution (21). Analogously we can introduce another collinear region $k^\mu \sim 1, l \sim n_-$. By the same argument we see that also this region has been already taken into account in (20).

In the hard region IBP identities provide a reduction of (19) to the set of integrals

$$\begin{aligned}
I_{b1,h} &= \int [dk][dl] \frac{1}{((k+p)^2-1)((k+p-q)^2-1)l^2(k+l)^2} \\
I_{b2,h} &= \int [dk][dl] \frac{1}{((k+p)^2-1)((k+p-q)^2-1)l^4(k+l)^2}.
\end{aligned} \tag{22}$$

These integrals can be evaluated via differential equations with respect to $\hat{s}$. By defining

$$\vec{I} = \begin{pmatrix} I_{b1,h} \\ I_{b2,h} \end{pmatrix} \tag{23}$$

and differentiating $\vec{I}$ with respect to $\hat{s}$ we obtain a differential equation of the form

$$\frac{d}{d\hat{s}}\vec{I} = h\vec{I} + \vec{g} \tag{24}$$

where $\vec{g}$ contains the integrals (A14) and (A15). We define the expansion in ϵ

$$\begin{aligned}
\vec{I} &= \sum_{i=-2}^{\infty} \vec{I}^{(i)}\epsilon^i \\
h &= \sum_{i=0}^{\infty} h^{(i)}\epsilon^i \\
\vec{g} &= \sum_{i=-2}^{\infty} \vec{g}^{(i)}\epsilon^i
\end{aligned} \tag{25}$$

and write (24) in the expanded form

$$\begin{aligned}
\frac{d}{d\hat{s}}\vec{I}^{(-2)} &= h^{(0)}\vec{I}^{(-2)} + \vec{g}^{(-2)} \\
\frac{d}{d\hat{s}}\vec{I}^{(-1)} &= h^{(0)}\vec{I}^{(-1)} + h^{(1)}\vec{I}^{(-2)} + \vec{g}^{(-1)} \\
\frac{d}{d\hat{s}}\vec{I}^{(0)} &= h^{(0)}\vec{I}^{(0)} + h^{(1)}\vec{I}^{(-1)} + h^{(2)}\vec{I}^{(-2)} + \vec{g}^{(0)}.
\end{aligned} \tag{26}$$

In our special case $h_{12}^{(0)} = 0$ such that (26) decouples and we can solve (26) by the common methods *separation of variables* and *variation of constants*. From Feynman parameterization we see that the limit $\hat{s} = 0$ does not lead to additional divergences in ϵ and can be used as initial condition for (26). Finally we obtain

$$\begin{aligned}
I_{b1,h} = \frac{1}{(4\pi)^4}\mu^{4\epsilon}\Bigg[&\frac{-1}{2\epsilon^2} + \frac{2\sqrt{\frac{4-\hat{s}}{\hat{s}}}\arcsin\frac{\sqrt{\hat{s}}}{2} - \frac{5}{2}}{\epsilon} + \frac{3\left(\hat{s}-3\right)\arcsin^2\frac{\sqrt{\hat{s}}}{2}}{\hat{s}-1} \\
&+ \frac{-5\pi^2\hat{s} - 114\hat{s} + 7\pi^2 + 114}{12\left(\hat{s}-1\right)} + \sqrt{\frac{4-\hat{s}}{\hat{s}}}\Bigg(\arcsin\frac{\sqrt{\hat{s}}}{2}\left(-2\ln\left(4-\hat{s}\right) + \ln\left(\hat{s}\right) + 10\right) \\
&+ \mathrm{Cl}_2\left(2\arcsin\frac{\sqrt{\hat{s}}}{2}\right) - 2\mathrm{Cl}_2\left(2\arcsin\frac{\sqrt{\hat{s}}}{2} + \pi\right)\Bigg)\Bigg] \\
I_{b2,h} = \frac{1}{(4\pi)^4}\mu^{4\epsilon}\Bigg[&\frac{6\arcsin^2\frac{\sqrt{\hat{s}}}{2} - \frac{\pi^2}{6}}{\epsilon} + \left(12\ln\left(1-\hat{s}\right) + 3\ln\left(\hat{s}\right)\right)\arcsin^2\frac{\sqrt{\hat{s}}}{2} \\
&+ 4\mathrm{Cl}_2\left(6\arcsin\frac{\sqrt{\hat{s}}}{2} + \pi\right)\arcsin\frac{\sqrt{\hat{s}}}{2} - \frac{\pi^2}{3}\ln\left(1-\hat{s}\right) - 3\mathrm{Cl}_3\left(2\arcsin\frac{\sqrt{\hat{s}}}{2}\right) \\
&+ 6\mathrm{Cl}_3\left(2\arcsin\frac{\sqrt{\hat{s}}}{2} + \pi\right) + \frac{2}{3}\mathrm{Cl}_3\left(6\arcsin\frac{\sqrt{\hat{s}}}{2} + \pi\right) + 3\zeta(3)\Bigg],
\end{aligned} \tag{27}$$

where $\mathrm{Cl}_2(\phi) = \Im\mathrm{Li}_2(e^{i\phi})$ and $\mathrm{Cl}_3(\phi) = \Re\mathrm{Li}_3(e^{i\phi})$.

D. Diagrams of Fig. 1c

The topology Fig. 1c comes with the master integrals

$$\begin{aligned} I_{c1} &= \int [dk][dl] \frac{1}{(l^2-z)((k+l)^2-z)((l+q)^2-z)(k+p-q)^2} \\ I_{c2} &= \int [dk][dl] \frac{1}{(l^2-z)^2((k+l)^2-z)((l+q)^2-z)(k+p-q)^2} \\ I_{c3} &= \int [dk][dl] \frac{1}{(l^2-z)((k+l)^2-z)^2((l+q)^2-z)(k+p-q)^2}. \end{aligned} \tag{28}$$

They all get leading power contributions from the hard region, where IBP identities lead to a further reduction of I_{c2} and I_{c3} to I_{c1}. I_{c1} can be calculated by a differential equation with respect to $\hat{s}$, which reads:

$$\frac{d}{d\hat{s}} I_{c1,h} = \epsilon \frac{2\hat{s}-1}{\hat{s}(1-\hat{s})} I_{c1,h} - \kappa(\mu,\epsilon) \frac{1}{\hat{s}(1-\hat{s})}, \tag{29}$$

where

$$\kappa(\mu,\epsilon) = \frac{\left(\mu^2 e^{\gamma_E}\right)^{2\epsilon}}{(4\pi)^4} e^{2i\pi\epsilon} \frac{\Gamma(-1+2\epsilon)\Gamma^3(1-\epsilon)}{\Gamma(2-3\epsilon)}. \tag{30}$$

The most general solution of (29) is given by

$$c\hat{s}^{-\epsilon}(1-\hat{s})^{-\epsilon} - \kappa(\mu,\epsilon)(1-\hat{s})^{-\epsilon} \left[\frac{{}_2\mathrm{F}_1(-\epsilon,\epsilon;1+\epsilon;\hat{s})}{\epsilon} + \frac{\hat{s}\,{}_2\mathrm{F}_1(1-\epsilon,1+\epsilon;2+\epsilon;\hat{s})}{1+\epsilon} \right], \tag{31}$$

where we have to determine c. We note that both $\hat{s}=0$ and $\hat{s}=1$ are no appropriate initial conditions. Hence we determine c by calculating the term proportional to $\hat{s}^{-\epsilon}$ in the expansion of $I_{c1,h}$ around $\hat{s}=0$. The Mellin-Barnes representation (see e.g. [31]) of $I_{c1,h}$ reads

$$\begin{aligned} I_{c1,h} = &-\frac{\left(\mu^2 e^{\gamma_E}\right)^{2\epsilon}}{(4\pi)^4} e^{2i\pi\epsilon} \int_{-i\infty}^{i\infty} dt\, \hat{s}^t \Gamma(-t)\Gamma(t+2\epsilon) \int_0^1 dx\, x^{-2\epsilon}(1-x)^t \\ &\times \int_0^1 d^2y\, y_1^{-1-\epsilon-t}(1-y_1)^{-\epsilon} y_2^{-2\epsilon-t}(1-y_2)^{-\epsilon}(1-y_1y_2)^t. \end{aligned} \tag{32}$$

We have to calculate the residue at $t=-\epsilon$ in (32), which arises due to the integration $\int_0^1 d^2y\, y_1^{-1-\epsilon-t}(\ldots)$ at $y_1=0$. So we can set $y_1=0$ in the ellipsis and obtain

$$I_{c1,h} = \hat{s}^{-\epsilon} \left[-\frac{\left(\mu^2 e^{\gamma_E}\right)^{2\epsilon}}{(4\pi)^4} e^{2i\pi\epsilon} \frac{\Gamma^2(\epsilon)\Gamma^3(1-\epsilon)}{(1-2\epsilon)\Gamma(2-3\epsilon)} \right] + \ldots, \tag{33}$$

where the ellipsis denotes integer powers of $\hat{s}$. Hence c reads

$$c = -\frac{\left(\mu^2 e^{\gamma_E}\right)^{2\epsilon}}{(4\pi)^4} e^{2i\pi\epsilon} \frac{\Gamma^2(\epsilon)\Gamma^3(1-\epsilon)}{(1-2\epsilon)\Gamma(2-3\epsilon)}. \tag{34}$$

In the collinear region $k^+, l^+ \sim 1$, $k_\perp, l_\perp \sim \sqrt{z}$, $k^-, l^- \sim z$ both I_{c2} and I_{c3} get a leading power contribution:

$$
\begin{aligned}
I_{c2,c} &= z^{-2\epsilon} \int [dk][dl] \frac{1}{(l^2-1)^2((k+l)^2-1)(2l^+q^- + \hat{s})(k^2 + 2k^-(p-q)^+)} = \\
&- \frac{(\mu^2 e^{\gamma_E})^{2\epsilon}}{(4\pi)^2} \frac{\Gamma^2(\epsilon)}{2(1-\epsilon)} \frac{z^{-2\epsilon}}{\hat{s}} \, {}_3\mathrm{F}_2 \left(1, 1, \epsilon; 2-\epsilon, 1+2\epsilon; \frac{\hat{s}-1}{\hat{s}}\right) \\
I_{c3,c} &= z^{-2\epsilon} \int [dk][dl] \frac{1}{(l^2-1)((k+l)^2-1)^2(2l^+q^- + \hat{s})(k^2 + 2k^-(p-q)^+)} = \\
&- \frac{(\mu^2 e^{\gamma_E})^{2\epsilon}}{(4\pi)^2} \frac{\Gamma^2(\epsilon)}{2(1-\epsilon)} \frac{z^{-2\epsilon}}{\hat{s}} \, {}_3\mathrm{F}_2 \left(1, 1, 1+\epsilon; 2-\epsilon, 1+2\epsilon; \frac{\hat{s}-1}{\hat{s}}\right),
\end{aligned} \tag{35}
$$

where ${}_3\mathrm{F}_2$ is given by

$$
{}_3\mathrm{F}_2(a_1, a_2, a_3; b_1, b_2; x) = \sum_{n=0}^{\infty} \frac{\Gamma(a_1+n)\Gamma(a_2+n)\Gamma(a_3+n)}{\Gamma(a_1)\Gamma(a_2)\Gamma(a_3)} \frac{\Gamma(b_1)\Gamma(b_2)}{\Gamma(b_1+n)\Gamma(b_2+n)} \frac{x^n}{n!}, \tag{36}
$$

and can be expanded in ϵ by the tools developed in [44, 45].

In the soft region $k^\mu + l^\mu \sim \sqrt{z}$ only I_{c3} contributes in leading power:

$$
I_{c3,s} = z^{-\epsilon} \int [dk][dl] \frac{1}{l^2(l+q)^2(l-p+q)^2(k^2-z)^2}, \tag{37}
$$

which is a product of two simple one-loop integrals. There are two further collinear regions $k + l \sim n_+$ and $k + l \sim n_-$, where I_{c3} obtains a leading power contribution. However by an argument similar to that given in the previous subsection we can show that these contributions have already been taken into account by (37).

As described above the subleading powers of (28) are obtained via differential equations with respect to z. Like in the previous cases the terms of the order $z^0 \ln z$ provide a check that we have taken all regions contributing at leading power consistently into account.

E. Diagrams of Fig. 1d

The topology in Fig. 1d comes with two sets of master integrals.

$$
\begin{aligned}
I_{d11} &= \int [dk][dl] \frac{1}{(l^2-z)((l-k)^2-z)((l-q)^2-z)((k-p)^2-1)} \\
I_{d12} &= \int [dk][dl] \frac{1}{(l^2-z)((l-k)^2-z)^2((l-q)^2-z)((k-p)^2-1)} \\
I_{d13} &= \int [dk][dl] \frac{1}{(l^2-z)((l-k)^2-z)((l-q)^2-z)^2((k-p)^2-1)} \\
I_{d14} &= \int [dk][dl] \frac{1}{(l^2-z)((l-k)^2-z)((l-q)^2-z)((k-p)^2-1)^2}
\end{aligned} \tag{38}
$$

and

$$
\begin{aligned}
I_{d21} &= \int [dk][dl] \frac{1}{k^2((l-k)^2-z)((l-q)^2-z)((k-p)^2-1)} \\
I_{d22} &= \int [dk][dl] \frac{1}{k^2((l-k)^2-z)((l-q)^2-z)^2((k-p)^2-1)} \\
I_{d23} &= \int [dk][dl] \frac{1}{k^2((l-k)^2-z)((l-q)^2-z)((k-p)^2-1)^2}.
\end{aligned} \tag{39}
$$

Let us consider the first set (38). In the hard region this set reduces by IBP identities to I_{d11} and I_{d12}. These integrals can be calculated by differential equations with respect to $\hat{s}$. We obtain a system of differential equations similar to (26) where we have to use $\hat{s}=1$ as initial condition because the integrals diverge at $\hat{s}=0$. The matrix $h^{(0)}$ has vanishing off-diagonal elements such that the system of differential equations decouples. In addition the $h^{(i)}$ contain only terms of the form $1/(1-\hat{s})$, $1/\hat{s}$ and $\hat{s}^n$. So we can reduce the integrals to harmonic polylogarithms, which were defined in [46]. The way to do this is very well described in Section 2.4 of [47]. Finally we used the program described in [48, 49] to convert harmonic polylogarithms into common functions like polylogarithms.

The soft region $l^\mu - k^\mu \sim \sqrt{z}$ leads to a leading power contribution of I_{d12}

$$
I_{d12,s} = z^{-\epsilon} \int [dk][dl] \frac{1}{k^2(k-q)^2((k-p)^2-1)(l^2-1)^2}, \tag{40}
$$

where we substituted $l \to l+k$. This integral is a product of (A5) and a simple one-loop tadpole integral.

The soft region $l^\mu - q^\mu \sim \sqrt{z}$ leads to a leading power contribution of I_{d13}

$$
I_{d13,s} = \frac{z^{-\epsilon}}{\hat{s}} \int [dk][dl] \frac{1}{k^2(k^2-1)(l^2-1)^2}, \tag{41}
$$

where we substituted $l \to l+q$. This integral is a product of two simple one-loop integrals.

Let us consider the second set of master integrals (39). In the hard region the set reduces via IBP identities to I_{d21}. We evaluated I_{d21} by a differential equation with respect to $\hat{s}$. Solving this differential equation is a straightforward calculation, which is analogous to the way we solved (29).

The soft region $l^\mu - q^\mu \sim \sqrt{z}$ leads to a leading power contribution of I_{d22}

$$
I_{d22,s} = z^{-\epsilon} \int [dk][dl] \frac{1}{k^2(k-q)^2((k-p)^2-1)(l^2-1)^2}, \tag{42}
$$

which coincides with (40).

Besides the leading power we also need the order z of I_{d21}. It is straightforward to calculate the order z contribution of the hard region by expanding the integrand of I_{d21} up to the order z. Finally the soft regions $l^\mu - k^\mu \sim \sqrt{z}$ and $l^\mu - q^\mu \sim \sqrt{z}$ contribute at order z. Since these regions do not overlap we have to take both of them into account. After an appropriate shift of l, I_{d21} can in both regions be cast into the form

$$I_{d21,s} = z^{1-\epsilon} \int [dk][dl] \frac{1}{k^2(k-q)^2((k-p)^2-1)(l^2-1)}, \tag{43}$$

which is similar to (40).

F. Diagrams of Fig. 1e and f

The integrals occurring in the diagrams of Fig. 1e reduce to (A2), (A11), (A12) and (A13). The topology of Fig. 1f factorizes trivially into two one-loop topologies, which have already been evaluated exactly in $\hat{s}$ in [14]. As already mentioned in Section II, Fig. 1f does not contribute to the form factors $F_{1,2}^{(7,9)}$ by definition; its effect is, however, absorbed into a modified Wilson coefficient C_9 as in [14].

IV. RESULTS

A. Results for the form factors $F_{1,2}^{(7,9)}$ in the high q^2 region

In Section III we calculated the two-loop diagrams in Fig. 1a –e which contribute to the form factors $F_{1,2}^{(7,9)}$ defined in (3). In addition, there are counterterm contributions which have to be taken into account. These counterterms are qualitatively the same as those discussed in Section III.B of [14]. Because its calculation in the high q^2-region is straightforward, we do not list their explicit results. We only stress that in the following results the c-quark mass is renormalized in the pole-scheme.

We calculated the renormalized form factors $F_{1,2}^{(7,9)}$ in the large q^2-region as expansions of the form $c_{nm}(\hat{s}) z^n \ln^m z$ ($n = 0, \frac{1}{2}, 1, \frac{3}{2}, \ldots$; $m = 0, 1, 2, \ldots$), keeping the full analytic dependence on $\hat{s}$ ($z = m_c^2/m_b^2$, $\hat{s} = q^2/m_b^2$). We included all orders up to z^{10}. To demonstrate the convergence of the power expansions, we show in Fig. 2 the form factors as functions of $\hat{s}$, where we include all orders up to z^6, z^8 and z^{10}. We use as default value $z = 0.1$ such

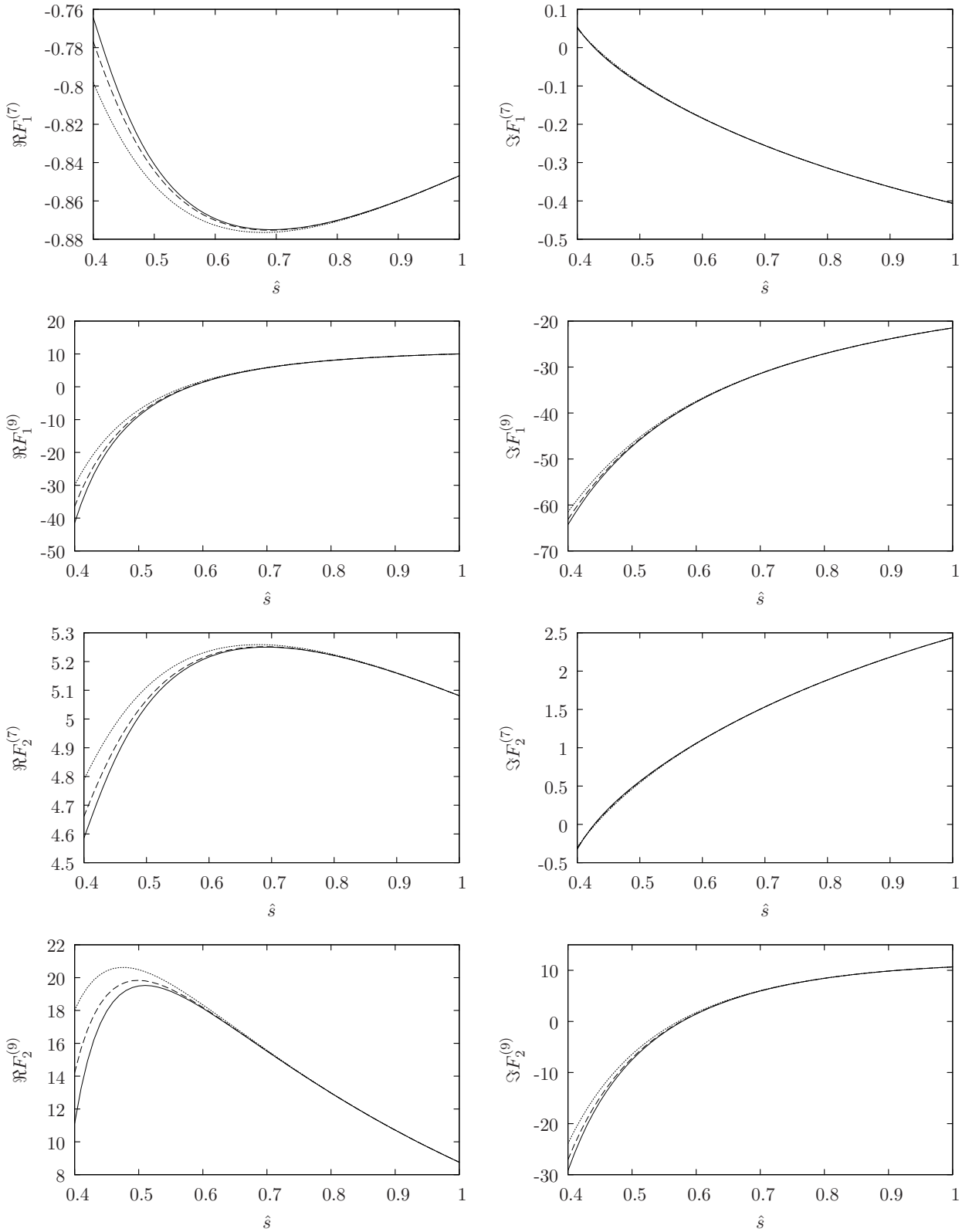

FIG. 2: Real and imaginary parts of the form factors $F_{1,2}^{(7,9)}$ as functions of $\hat{s}$. To demonstrate the convergence of the expansion in z we included all orders up to z^6, z^8 and z^{10} in the dotted, dashed and solid lines respectively. We put $\mu = m_b$ and used the default value $z = 0.1$.

$\sqrt{z}$	$\hat{s}$	$F_1^{(7)}$	$F_2^{(7)}$
0.25	0.6	$-0.928 - 0.408i - 0.856\ell$	$5.57 + 2.45i + 5.14\ell$
	0.7	$-0.909 - 0.458i - 0.856\ell$	$5.45 + 2.75i + 5.14\ell$
	0.8	$-0.888 - 0.500i - 0.856\ell$	$5.33 + 3.00i + 5.14\ell$
	0.9	$-0.867 - 0.535i - 0.856\ell$	$5.20 + 3.21i + 5.14\ell$
0.27	0.6	$-0.919 - 0.347i - 0.856\ell$	$5.52 + 2.08i + 5.14\ell$
	0.7	$-0.905 - 0.402i - 0.856\ell$	$5.43 + 2.41i + 5.14\ell$
	0.8	$-0.888 - 0.449i - 0.856\ell$	$5.33 + 2.69i + 5.14\ell$
	0.9	$-0.869 - 0.488i - 0.856\ell$	$5.21 + 2.93i + 5.14\ell$
0.29	0.6	$-0.904 - 0.280i - 0.856\ell$	$5.42 + 1.68i + 5.14\ell$
	0.7	$-0.896 - 0.342i - 0.856\ell$	$5.38 + 2.05i + 5.14\ell$
	0.8	$-0.883 - 0.393i - 0.856\ell$	$5.30 + 2.36i + 5.14\ell$
	0.9	$-0.867 - 0.437i - 0.856\ell$	$5.20 + 2.62i + 5.14\ell$
0.31	0.6	$-0.879 - 0.208i - 0.856\ell$	$5.28 + 1.25i + 5.14\ell$
	0.7	$-0.881 - 0.277i - 0.856\ell$	$5.29 + 1.66i + 5.14\ell$
	0.8	$-0.874 - 0.334i - 0.856\ell$	$5.24 + 2.00i + 5.14\ell$
	0.9	$-0.862 - 0.382i - 0.856\ell$	$5.17 + 2.29i + 5.14\ell$
0.33	0.6	$-0.842 - 0.130i - 0.856\ell$	$5.05 + 0.779i + 5.14\ell$
	0.7	$-0.858 - 0.207i - 0.856\ell$	$5.15 + 1.24i + 5.14\ell$
	0.8	$-0.859 - 0.269i - 0.856\ell$	$5.15 + 1.62i + 5.14\ell$
	0.9	$-0.853 - 0.322i - 0.856\ell$	$5.12 + 1.93i + 5.14\ell$

TABLE I: Numerical results for the form factors $F_{1,2}^{(7)}$, for different values of z and $\hat{s}$ ($\ell = \ln \frac{\mu}{m_b}$).

that the $c\bar{c}$-threshold is located at $\hat{s} = 0.4$. One sees from the figures that far away from the $c\bar{c}$-threshold, i.e. for $\hat{s} > 0.6$, the expansions for all form factors are well behaved.

In Tab. I,II we list numerical values of the form factors for different values of z and $\hat{s}$, retaining the dependence on the renormalization scale μ. We compared our values in Tab. I,II with the numerical values [50] that were used in [1]. We obtain nearly perfect agreement, i.e. the difference is always smaller than 1%.

Unfortunately, the form factors are too lengthy to be given explicitly in this paper.

$\sqrt{z}$	$\hat{s}$	$F_1^{(9)}$	$F_2^{(9)}$
0.25	0.6	$8.72 - 22.9i + (-5.47 - 3.23i)\ell - 1.05\ell^2$	$13.2 + 13.6i + (22.1 + 19.4i)\ell + 6.32\ell^2$
	0.7	$9.53 - 19.8i + (-5.13 - 3.31i)\ell - 1.05\ell^2$	$10.3 + 14.5i + (20.1 + 19.9i)\ell + 6.32\ell^2$
	0.8	$9.92 - 17.5i + (-4.86 - 3.36i)\ell - 1.05\ell^2$	$7.88 + 14.8i + (18.5 + 20.2i)\ell + 6.32\ell^2$
	0.9	$10.1 - 15.8i + (-4.64 - 3.40i)\ell - 1.05\ell^2$	$5.93 + 14.8i + (17.2 + 20.4i)\ell + 6.32\ell^2$
0.27	0.6	$7.65 - 26.6i + (-5.66 - 3.11i)\ell - 1.05\ell^2$	$15.0 + 10.9i + (23.3 + 18.7i)\ell + 6.32\ell^2$
	0.7	$9.07 - 22.7i + (-5.29 - 3.23i)\ell - 1.05\ell^2$	$12.0 + 12.6i + (21.1 + 19.4i)\ell + 6.32\ell^2$
	0.8	$9.78 - 20.0i + (-5.00 - 3.30i)\ell - 1.05\ell^2$	$9.44 + 13.3i + (19.3 + 19.8i)\ell + 6.32\ell^2$
	0.9	$10.2 - 17.9i + (-4.76 - 3.35i)\ell - 1.05\ell^2$	$7.35 + 13.6i + (17.9 + 20.1i)\ell + 6.32\ell^2$
0.29	0.6	$5.76 - 31.0i + (-5.88 - 2.95i)\ell - 1.05\ell^2$	$16.6 + 7.46i + (24.6 + 17.7i)\ell + 6.32\ell^2$
	0.7	$8.11 - 26.2i + (-5.47 - 3.12i)\ell - 1.05\ell^2$	$13.6 + 10.1i + (22.2 + 18.7i)\ell + 6.32\ell^2$
	0.8	$9.32 - 22.8i + (-5.15 - 3.22i)\ell - 1.05\ell^2$	$11.0 + 11.5i + (20.3 + 19.3i)\ell + 6.32\ell^2$
	0.9	$9.98 - 20.3i + (-4.89 - 3.29i)\ell - 1.05\ell^2$	$8.81 + 12.2i + (18.7 + 19.7i)\ell + 6.32\ell^2$
0.31	0.6	$2.65 - 35.9i + (-6.12 - 2.74i)\ell - 1.05\ell^2$	$17.9 + 3.06i + (26.1 + 16.4i)\ell + 6.32\ell^2$
	0.7	$6.46 - 30.1i + (-5.67 - 2.98i)\ell - 1.05\ell^2$	$15.1 + 7.05i + (23.4 + 17.9i)\ell + 6.32\ell^2$
	0.8	$8.41 - 26.0i + (-5.32 - 3.12i)\ell - 1.05\ell^2$	$12.5 + 9.24i + (21.3 + 18.7i)\ell + 6.32\ell^2$
	0.9	$9.50 - 23.0i + (-5.04 - 3.21i)\ell - 1.05\ell^2$	$10.3 + 10.5i + (19.6 + 19.3i)\ell + 6.32\ell^2$
0.33	0.6	$-2.28 - 41.7i + (-6.39 - 2.45i)\ell - 1.05\ell^2$	$18.4 - 2.61i + (27.7 + 14.7i)\ell + 6.32\ell^2$
	0.7	$3.84 - 34.6i + (-5.89 - 2.79i)\ell - 1.05\ell^2$	$16.3 + 3.20i + (24.7 + 16.8i)\ell + 6.32\ell^2$
	0.8	$6.90 - 29.7i + (-5.51 - 2.99i)\ell - 1.05\ell^2$	$13.9 + 6.42i + (22.4 + 17.9i)\ell + 6.32\ell^2$
	0.9	$8.60 - 26.1i + (-5.20 - 3.12i)\ell - 1.05\ell^2$	$11.7 + 8.31i + (20.5 + 18.7i)\ell + 6.32\ell^2$

TABLE II: Numerical results for the form factors $F_{1,2}^{(9)}$, for different values of z and $\hat{s}$ ($\ell = \ln \frac{\mu}{m_b}$).

Hence, the complete analytical results are attached to the source-code files of the present paper at `www.arxiv.org`. The Mathematica file `F_high.m` contains the expressions for `F17HighRe`, `F17HighIm`, `F19HighRe`, `F19HighIm`, `F27HighRe`, `F27HighIm`, `F29HighRe` and `F29HighIm`, which represent the real and imaginary part of the form factors $F_{1,2}^{(7,9)}$ in the high $\hat{s}$ region; they are defined in terms of `muh`, `z` and `sh` standing for μ/m_b, z and $\hat{s}$ respectively. Additionally this file contains the expressions for `DeltaF19HighRe`, `DeltaF19HighIm`, `DeltaF29HighRe` and `DeltaF29HighIm`, which have to be added to the pole-scheme form fac-

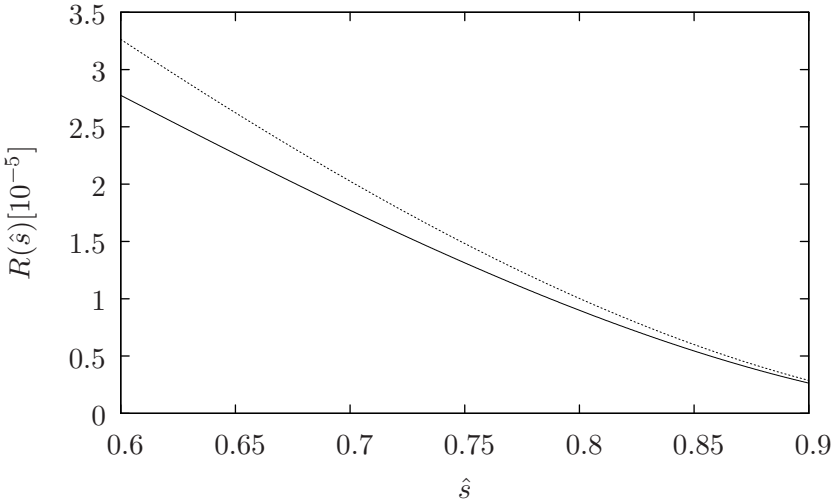

FIG. 3: Perturbative part of $R(\hat{s})$ at NNLL. The solid line represents the NNLL result, whereas in the dotted line the order α_s corrections to the matrix elements associated with $O_{1,2}$ are switched off. We use $\mu = m_b$. See text for details.

tors in order to switch from the pole-scheme to the $\overline{\text{MS}}$-scheme of the c-quark mass. For completeness we also provide the file `F_low.m`, which contains the analogous expressions in the low $\hat{s}$ region (`F17LowRe` etc.) taken from [14]. For numerical purposes we also provide the c++ header files `F_1.h` and `F_2.h` that contain the analogously defined functions

```
double F_17re(double muh, double z, double sh),
double F_17im(double muh, double z, double sh),  etc.
```

valid in both high and low $\hat{s}$ region. These files need for numerical evaluation of the harmonic polylogarithms the header file `hpl.h`, which we provide at the same place.

B. Impact on the dilepton invariant mass spectrum in the high q^2 region

In this section we briefly discuss the impact of the form factors $F_{1,2}^{(7,9)}$ calculated in this paper on the q^2-spectrum at high values of q^2. To this end, we consider as in [14] the perturbative part of the ratio

$$R(\hat{s}) = \frac{1}{\Gamma(\bar{B} \to X_c e^- \bar{\nu}_e)} \frac{d\Gamma(\bar{B} \to X_s \ell^+ \ell^-)}{d\hat{s}}, \tag{44}$$

where the formulas for the decay rates $\Gamma(b \to X_c e^- \bar{\nu}_e)$ and $d\Gamma(b \to X_s \ell^+ \ell^-)/d\hat{s}$ can be found e.g. in Section VI of [14]. The parameterization of $d\Gamma(b \to X_s \ell^+ \ell^-)/d\hat{s}$ as specified in (89) and (90) of [14] is also valid in the high q^2 region. All the ingredients contained in these two eqs. are available for arbitrary q^2, except $F_{1,2,8}^{(7,9)}$. The expressions for $F_{1,2}^{(7,9)}$ were derived in the previous sections of this paper in the high q^2 range. The calculations of the renormalized form factors $F_8^{(7,9)}$ is much easier and we therefore immediately give the results (valid for arbitrary $\hat{s} \in [0,1]$):

$$\begin{aligned} F_8^{(7)} = \; & \frac{4\pi^2}{27}\frac{(2+\hat{s})}{(1-\hat{s})^4} - \frac{4}{9}\frac{(11-16\hat{s}+8\hat{s}^2)}{(1-\hat{s})^2} - \frac{8}{9}\frac{\sqrt{\hat{s}}\sqrt{4-\hat{s}}}{(1-\hat{s})^3}(9-5\hat{s}+2\hat{s}^2)\arcsin\left(\frac{\sqrt{\hat{s}}}{2}\right) \\ & -\frac{16}{3}\frac{2+\hat{s}}{(1-\hat{s})^4}\arcsin^2\left(\frac{\sqrt{\hat{s}}}{2}\right) - \frac{8\hat{s}}{9(1-\hat{s})}\ln\hat{s} - \frac{32}{9}\ln\frac{\mu}{m_b} - \frac{8}{9}\pi\, i \end{aligned} \tag{45}$$

$$\begin{aligned} F_8^{(9)} = \; & -\frac{8\pi^2}{27}\frac{(4-\hat{s})}{(1-\hat{s})^4} + \frac{8}{9}\frac{(5-2\hat{s})}{(1-\hat{s})^2} + \frac{16}{9}\frac{\sqrt{4-\hat{s}}}{\sqrt{\hat{s}}\,(1-\hat{s})^3}(4+3\hat{s}-\hat{s}^2)\arcsin\left(\frac{\sqrt{\hat{s}}}{2}\right) \\ & +\frac{32}{3}\frac{(4-\hat{s})}{(1-\hat{s})^4}\arcsin^2\left(\frac{\sqrt{\hat{s}}}{2}\right) + \frac{16}{9(1-\hat{s})}\ln\hat{s} \end{aligned} \tag{46}$$

Fig. 3 shows $R(\hat{s})$ defined in (44), where we set $\mu = 5$ GeV and used $\sqrt{z} = m_{c,\text{pole}}/m_{b,\text{pole}} = 0.29$. We used the pole-mass for the b-quark and the $\overline{\text{MS}}$-mass for the top-quark and set $m_{b,\text{pole}} = 4.8$ GeV and $m_t(m_t) = 163$ GeV [51]. We neglected the finite bremsstrahlung corrections calculated in [15]. From Fig. 3 we conclude that for $\mu = m_b$ the contributions of the form factors $F_{1,2}^{(7,9)}$ lead to corrections of the order $10\% - 15\%$ at the level of the perturbative part of the normalized q^2 spectrum $R(\hat{s})$. Integrating $R(\hat{s})$ over the high $\hat{s}$ region, we define

$$R_{\text{high}} = \int_{0.6}^{1} d\hat{s}\, R(\hat{s}). \tag{47}$$

Fig. 4 shows the dependence of the perturbative part of R_{high} on the renormalization scale. We obtain

$$R_{\text{high,pert}} = (0.43 \pm 0.01(\mu)) \times 10^{-5}, \tag{48}$$

where we determined the error by varying μ between 2 GeV and 10 GeV. The corrections due to the form factors $F_{1,2}^{(7,9)}$ lead to a decrease of the scale dependence to 2%.

We should mention at this point that a normalization different from the one in (44) has been proposed in [24]: By normalizing the $\bar{B} \to X_s \ell^+ \ell^-$ decay rate to the semileptonic $\bar{B} \to$

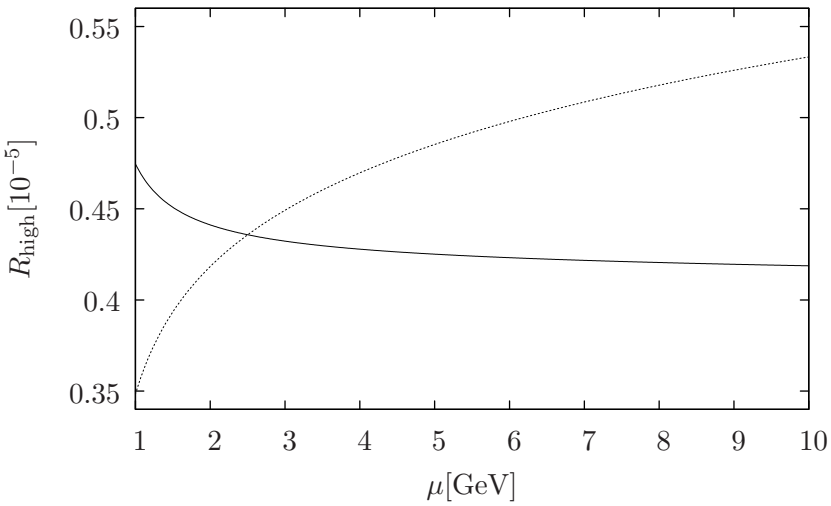

FIG. 4: Perturbative part of $R_{\rm high}$ as function of the renormalization scale μ at NNLL. The solid line represents the NNLL result, whereas in the dotted line the order α_s corrections to the matrix elements associated with $O_{1,2}$ are switched off. See text for details.

$X_u e^- \bar{\nu}_e$ decay rate with the same cut on q^2, the large theoretical uncertainties due to power corrections can be significantly reduced. It was shown explicitly in a recent phenomenological update [26] that the uncertainties from the poorly known $O(1/m_b^3)$ power corrections are then under control.

V. CONCLUSIONS

We calculated for the first time the NNLL virtual QCD corrections of the matrix elements of O_1 and O_2 in the high q^2 region as analytic functions of q^2 and m_c. While keeping the full analytic dependence on q^2, we evaluated the matrix elements as an expansion in z up to the 10th power, which is numerically stable for $\hat{s} > 0.6$. Making extensive use of differential equation techniques, we fully automatized the reduction of the higher order expansion coefficients to the leading and first subleading power, which were obtained via the method of regions.

Comparing our results for these matrix elements with those of a previous work where the master integrals were calculated numerically [1], we obtain an agreement up to 1%. Likewise in coincidence with [1], we find that the corrections calculated in the present paper lead to a decrease of the perturbative part of the q^2-spectrum by $10\% - 15\%$ relative to a NNLL

result where these contributions are not taken into account and reduce the renormalization scale uncertainty to 2%.

We provide the rather lengthy results of our calculation in electronic form as Mathematica files and for numerical purposes also as c++ files.

VI. ACKNOWLEDGMENTS

We would like to thank Thorsten Ewerth for initiating this project and for collaboration at an early stage. We also thank H. Asatrian and U. Haisch for helpful discussions. This work is partially supported by the Swiss National Foundation as well as EC-Contract MRTN-CT-2006-035482 (FLAVIAnet). The Center for Research and Education in Fundamental Physics (Bern) is supported by the "Innovations- und Kooperationsprojekt C-13 of the Schweizerische Universitätskonferenz SUK/CRUS".

APPENDIX A: COMMON MASTER INTEGRALS

All integrals are evaluated in $d = 4-2\epsilon$ dimensions. In the following notation we suppress the positive imaginary part $+i0$ of the denominators. The integration measure is defined as

$$[dk] = \left(\frac{\mu^2}{4\pi}e^{\gamma_E}\right)^{\epsilon} \frac{d^d k}{(2\pi)^d}. \tag{A1}$$

1. One-loop integrals

a. *2-point integral with two massive lines*

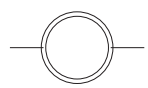

$$= \int [dk] \frac{1}{(k^2-m^2)((k+q)^2-m^2)} \tag{A2}$$

The double line denotes the massive propagator. We evaluate (A2) in the two regions $q^2 < 4m^2$ and $q^2 > 4m^2$. In the latter one we need the integral in an expansion in m^2/q^2. Using Mellin-Barnes representation [28, 52] it is easily seen that we can cast (A2) into the following form:

$$\frac{i}{(4\pi)^2}\left(\frac{\mu^2 e^{\gamma_E}}{q^2}\right)^{\epsilon} \frac{1}{2\pi i}\int_{-i\infty}^{i\infty} dt \left(\frac{m^2}{q^2}\right)^t e^{i\pi(t+\epsilon)} \frac{\Gamma(-t)\Gamma(t+\epsilon)\Gamma^2(1-t-\epsilon)}{\Gamma(2-2t-2\epsilon)}, \tag{A3}$$

where the integration contour over t has to be chosen such that $-\epsilon < \Re(t) < 0$. The poles on the right hand side of the contour are located at $t = n$ and $t = n+1-\epsilon$ where $n \in \mathbb{N}_0$. By closing the integration contour to the right we obtain the power expansion in m^2/q^2.

Now let us consider the region $q^2 < 4m^2$. Up to order ϵ the integral reads:

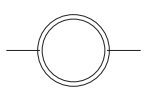

$$= \frac{i}{(4\pi)^2}\left(\frac{\mu^2}{m^2}\right)^{\epsilon} \times$$
$$\left[\frac{1}{\epsilon} + \sqrt{\frac{4-\hat{x}}{\hat{x}}}\arcsin\frac{\sqrt{\hat{x}}}{2} + \right.$$
$$\left.\epsilon\left(4 + \frac{\pi^2}{12} + \sqrt{\frac{4-\hat{x}}{\hat{x}}}\arcsin\frac{\sqrt{\hat{x}}}{2}\left(-4+2\ln(4-\hat{x})\right) + 2\sqrt{\frac{4-\hat{x}}{\hat{x}}}\mathrm{Cl}_2\left(2\arcsin\frac{\sqrt{\hat{x}}}{2}+\pi\right)\right)\right], \tag{A4}$$

where we defined $\hat{x} = q^2/m^2$ and $\mathrm{Cl}_2(\phi) = \Im\mathrm{Li}_2(e^{i\phi})$.

b. 3-point integral with one massive line

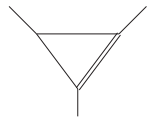

$$= \int [dk] \frac{1}{k^2(k+q)^2((k+p)^2-m^2)}, \tag{A5}$$

where

$$p^2 = m^2, \quad q^2 = \hat{x}m^2 \quad \text{and} \quad \hat{x} < 1. \tag{A6}$$

The integral is evaluated to

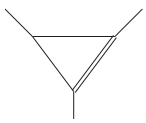

$$= \frac{i}{(4\pi)^2}\left(\frac{\mu^2 e^{\gamma_E}}{m^2}\right)^{\epsilon} \frac{1}{m^2}\frac{\Gamma(\epsilon)}{\Gamma(2-2\epsilon)}$$
$$\times \left[\Gamma(1-2\epsilon)\,{}_2\mathrm{F}_1(1,1;2-2\epsilon;1-\hat{x}) - \hat{x}^{-\epsilon}e^{i\pi\epsilon}\Gamma^2(1-\epsilon)\,{}_2\mathrm{F}_1(1,1-\epsilon;2-2\epsilon;1-\hat{x})\right], \tag{A7}$$

with ${}_2\mathrm{F}_1$ given by (11).

c. 3-point integral with two massive lines

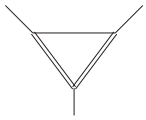

$$= \int [dk] \frac{1}{k^2((k+p)^2-m^2)((k+p-q)^2-m^2)}, \tag{A8}$$

where

$$p^2 = m^2, \quad q^2 = \hat{x}m^2, \quad (p-q)^2 = 0 \qquad q^2 < 4m^2. \tag{A9}$$

The expansion in ϵ of (A8) reads

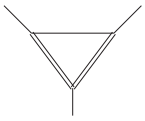

$$= \frac{i}{(4\pi)^2}\left(\frac{\mu^2}{m^2}\right)^{\epsilon} \frac{1}{m^2(1-\hat{x})}\times$$
$$\Bigg[-\frac{\pi^2}{6} + 6\arcsin^2\frac{\sqrt{\hat{x}}}{2} +$$
$$\epsilon\Bigg(12\ln(1-\hat{x})\arcsin^2\frac{\sqrt{\hat{x}}}{2} + 4\mathrm{Cl}_2\left(6\arcsin\frac{\sqrt{\hat{x}}}{2}+\pi\right)\arcsin\frac{\sqrt{\hat{x}}}{2} -$$
$$\frac{1}{3}\pi^2\ln(1-\hat{x}) + 6\mathrm{Cl}_3\left(2\arcsin\frac{\sqrt{\hat{x}}}{2}+\pi\right) + \frac{2}{3}\mathrm{Cl}_3\left(6\arcsin\frac{\sqrt{\hat{x}}}{2}+\pi\right) + 2\zeta(3)\Bigg)\Bigg], \tag{A10}$$

where $\mathrm{Cl}_3(\phi) = \Re\mathrm{Li}_3(e^{i\phi})$

2. Two-loop integrals

a. *Two massive lines*

We need the following three sunrise diagrams in an expansion in m^2/q^2. So as above we give the Mellin-Barnes representation, from where the expansion can be easily derived.

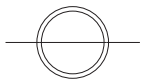

$$= \int [dk][dl] \frac{1}{(k+q)^2(l^2-m^2)((k+l)^2-m^2)} =$$
$$-\frac{1}{(4\pi)^4} q^2 \left(\frac{\mu^2 e^{2\gamma_E}}{q^2}\right)^{\epsilon} \Gamma(1-\epsilon) \frac{1}{2\pi i} \int_{-i\infty}^{i\infty} dt \left(\frac{m^2}{q^2}\right)^t e^{i\pi(2\epsilon+t)} \times$$
$$\frac{\Gamma(-t)\Gamma(t-1+2\epsilon)\Gamma^2(1-\epsilon-t)\Gamma(2-2\epsilon-t)}{\Gamma(2-2\epsilon-2t)\Gamma(3-3\epsilon-t)}. \tag{A11}$$

The residues we have to take into account are located at n, $n+1-\epsilon$ and $n+2-2\epsilon$ with $n \in \mathbb{N}_0$.

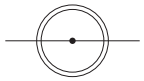

$$= \int [dk][dl] \frac{1}{\left[(k+q)^2\right]^2 (l^2-m^2)((k+l)^2-m^2)} =$$
$$-\frac{1}{(4\pi)^4} \left(\frac{\mu^2 e^{2\gamma_E}}{q^2}\right)^{\epsilon} \Gamma(-\epsilon) \frac{1}{2\pi i} \int_{-i\infty}^{i\infty} dt \left(\frac{m^2}{q^2}\right)^t e^{i\pi(2\epsilon+t)} \times$$
$$\frac{\Gamma(-t)\Gamma(t+2\epsilon)\Gamma^2(1-\epsilon-t)\Gamma(2-2\epsilon-t)}{\Gamma(2-2\epsilon-2t)\Gamma(2-3\epsilon-t)}. \tag{A12}$$

The dotted line denotes a propagator that has to be taken squared. The residues are located at n, $n+1-\epsilon$, $n+2-2\epsilon$, $n \in \mathbb{N}_0$.

$$= \int [dk][dl] \frac{1}{(k+q)^2(l^2-m^2)^2((k+l)^2-m^2)} =$$
$$-\frac{1}{(4\pi)^4} \left(\frac{\mu^2 e^{2\gamma_E}}{q^2}\right)^{\epsilon} \Gamma(1-\epsilon) \frac{1}{2\pi i} \int_{-i\infty}^{i\infty} dt \left(\frac{m^2}{q^2}\right)^t e^{i\pi(2\epsilon+t)} \times$$
$$\frac{\Gamma(-t)\Gamma(t+2\epsilon)\Gamma(-\epsilon-t)\Gamma(1-\epsilon-t)\Gamma(1-2\epsilon-t)}{\Gamma(1-2\epsilon-2t)\Gamma(2-3\epsilon-t)}, \tag{A13}$$

with the residues located at n, $n-\epsilon$, $n+1-\epsilon$, $n \in \mathbb{N}_0$.

b. *Three massive lines*

We need the following three integrals in an expansion in m^2/M^2. Therefore we give their Mellin-Barnes representation.

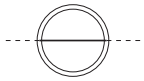

$$= \int [dk][dl] \frac{1}{(k^2-M^2)(l^2-m^2)^2((k+l)^2-m^2)} =$$
$$\frac{1}{(4\pi)^4} M^2 \left(\frac{\mu^2 e^{2\gamma_E}}{M^2}\right)^{\epsilon} \frac{1}{2\pi i} \int_{-i\infty}^{i\infty} dt \left(\frac{m^2}{M^2}\right)^t \times$$
$$\frac{\Gamma(-t)\Gamma(t-1+2\epsilon)\Gamma^2(1-\epsilon-t)\Gamma(\epsilon+t)\Gamma(2-2\epsilon-t)}{\Gamma(2-2\epsilon-2t)\Gamma(2-\epsilon)}, \tag{A14}$$

with the residues located at n, $n+1-\epsilon$, $n+2-2\epsilon$, $n \in \mathbb{N}_0$.

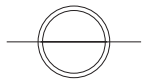

$$= \int [dk][dl] \frac{1}{((k+p)^2-M^2)(l^2-m^2)((k+l)^2-m^2)} =$$
$$\frac{1}{(4\pi)^4} M^2 \left(\frac{\mu^2 e^{2\gamma_E}}{M^2}\right)^{\epsilon} \frac{1}{2\pi i} \int_{-i\infty}^{i\infty} dt \left(\frac{m^2}{M^2}\right)^t \times$$
$$\frac{\Gamma(-t)\Gamma(t-1+2\epsilon)\Gamma^2(1-\epsilon-t)\Gamma(\epsilon+t)\Gamma(3-4\epsilon-2t)}{\Gamma(2-2\epsilon-2t)\Gamma(3-3\epsilon-t)}, \tag{A15}$$

with $p^2 = M^2$ and the residues located at n, $n+1-\epsilon$, $n/2+3/2-2\epsilon$, $n \in \mathbb{N}_0$.

$$= \int [dk][dl] \frac{1}{((k+p)^2-M^2)(l^2-m^2)^2((k+l)^2-m^2)} =$$
$$-\frac{1}{(4\pi)^4} \left(\frac{\mu^2 e^{2\gamma_E}}{M^2}\right)^{\epsilon} \frac{1}{2\pi i} \int_{-i\infty}^{i\infty} dt \left(\frac{m^2}{M^2}\right)^t \times$$
$$\frac{\Gamma(-t)\Gamma(t+2\epsilon)\Gamma(-\epsilon-t)\Gamma(1-\epsilon-t)\Gamma(1+\epsilon+t)\Gamma(1-4\epsilon-2t)}{\Gamma(1-2\epsilon-2t)\Gamma(2-3\epsilon-t)}, \tag{A16}$$

with $p^2 = M^2$ and the residues located at n, $n+1-\epsilon$, $n/2+1/2-2\epsilon$, $n \in \mathbb{N}_0$.

[1] A. Ghinculov, T. Hurth, G. Isidori and Y. P. Yao, Nucl. Phys. **B685**, 351 (2004), [hep-ph/0312128].

[2] B. Grinstein, M. J. Savage and M. B. Wise, Nucl. Phys. **B319**, 271 (1989).

[3] M. Misiak, Nucl. Phys. **B393**, 23 (1993), [Erratum-ibid. B **439** (1995) 461].

[4] A. J. Buras and M. Münz, Phys. Rev. **D52**, 186 (1995), [hep-ph/9501281].

[5] G. Buchalla, A. J. Buras and M. E. Lautenbacher, Rev. Mod. Phys. **68**, 1125 (1996), [hep-ph/9512380].

[6] K. Adel and Y.-P. Yao, Phys. Rev. **D49**, 4945 (1994), [hep-ph/9308349].

[7] C. Greub and T. Hurth, Phys. Rev. **D56**, 2934 (1997), [hep-ph/9703349].

[8] C. Bobeth, M. Misiak and J. Urban, Nucl. Phys. **B574**, 291 (2000), [hep-ph/9910220].

[9] K. G. Chetyrkin, M. Misiak and M. Munz, Phys. Lett. **B400**, 206 (1997), [hep-ph/9612313].

[10] P. Gambino, M. Gorbahn and U. Haisch, Nucl. Phys. **B673**, 238 (2003), [hep-ph/0306079].

[11] C. Bobeth, P. Gambino, M. Gorbahn and U. Haisch, JHEP **04**, 071 (2004), [hep-ph/0312090].

[12] M. Gorbahn and U. Haisch, Nucl. Phys. **B713**, 291 (2005), [hep-ph/0411071].

[13] H. H. Asatrian, H. M. Asatrian, C. Greub and M. Walker, Phys. Lett. **B507**, 162 (2001), [hep-ph/0103087].

[14] H. H. Asatryan, H. M. Asatrian, C. Greub and M. Walker, Phys. Rev. **D65**, 074004 (2002), [hep-ph/0109140].

[15] H. H. Asatryan, H. M. Asatrian, C. Greub and M. Walker, Phys. Rev. **D66**, 034009 (2002), [hep-ph/0204341].

[16] A. Ghinculov, T. Hurth, G. Isidori and Y. P. Yao, Nucl. Phys. **B648**, 254 (2003), [hep-ph/0208088].

[17] H. M. Asatrian, K. Bieri, C. Greub and A. Hovhannisyan, Phys. Rev. **D66**, 094013 (2002), [hep-ph/0209006].

[18] A. F. Falk, M. E. Luke and M. J. Savage, Phys. Rev. **D49**, 3367 (1994), [hep-ph/9308288].

[19] A. Ali, G. Hiller, L. T. Handoko and T. Morozumi, Phys. Rev. **D55**, 4105 (1997), [hep-ph/9609449].

[20] J.-W. Chen, G. Rupak and M. J. Savage, Phys. Lett. **B410**, 285 (1997), [hep-ph/9705219].

[21] G. Buchalla, G. Isidori and S. J. Rey, Nucl. Phys. **B511**, 594 (1998), [hep-ph/9705253].

[22] G. Buchalla and G. Isidori, Nucl. Phys. **B525**, 333 (1998), [hep-ph/9801456].

[23] C. W. Bauer and C. N. Burrell, Phys. Rev. **D62**, 114028 (2000), [hep-ph/9911404].

[24] Z. Ligeti and F. J. Tackmann, Phys. Lett. **B653**, 404 (2007), [arXiv:0707.1694].

[25] T. Huber, E. Lunghi, M. Misiak and D. Wyler, Nucl. Phys. **B740**, 105 (2006), [hep-ph/0512066].

[26] T. Huber, T. Hurth and E. Lunghi, Nucl. Phys. **B802**, 40 (2008), [arXiv:0712.3009].

[27] T. Huber, T. Hurth and E. Lunghi, [0807.1940].

[28] V. A. Smirnov, Springer Tracts Mod. Phys. **177**, 1 (2002).

[29] S. G. Gorishnii, Nucl. Phys. **B319**, 633 (1989).

[30] M. Beneke and V. A. Smirnov, Nucl. Phys. **B522**, 321 (1998), [hep-ph/9711391].

[31] V. A. Smirnov, Commun. Math. Phys. **134**, 109 (1990).

[32] E. Remiddi, Nuovo Cim. **A110**, 1435 (1997), [hep-th/9711188].

[33] V. Pilipp, Nucl. Phys. **B794**, 154 (2008), [arXiv:0709.3214].

[34] V. Pilipp, JHEP **09**, 135 (2008), [arXiv:0808.2555].

[35] R. Boughezal, M. Czakon and T. Schutzmeier, JHEP **09**, 072 (2007), [arXiv:0707.3090].

[36] C. W. Bauer, Z. Ligeti and M. E. Luke, Phys. Lett. B **479** (2000) 395, [arXiv:hep-ph/0002161].

[37] M. Neubert, JHEP **0007**, 022 (2000), [arXiv:hep-ph/0006068].

[38] G. Passarino and M. J. G. Veltman, Nucl. Phys. **B160**, 151 (1979).

[39] K. G. Chetyrkin and F. V. Tkachov, Nucl. Phys. **B192**, 159 (1981).

[40] F. V. Tkachov, Phys. Lett. **B100**, 65 (1981).

[41] S. Laporta, Int. J. Mod. Phys. **A15**, 5087 (2000), [hep-ph/0102033].

[42] C. Anastasiou and A. Lazopoulos, JHEP **07**, 046 (2004), [hep-ph/0404258].

[43] A. V. Kotikov, Phys. Lett. **B254**, 158 (1991).

[44] T. Huber and D. Maitre, Comput. Phys. Commun. **175**, 122 (2006), [hep-ph/0507094].

[45] T. Huber and D. Maitre, Comput. Phys. Commun. **178**, 755 (2008), [arXiv:0708.2443].

[46] E. Remiddi and J. A. M. Vermaseren, Int. J. Mod. Phys. **A15**, 725 (2000), [hep-ph/9905237].

[47] G. Bell, [arXiv:0705.3133].

[48] D. Maitre, Comput. Phys. Commun. **174**, 222 (2006), [hep-ph/0507152].

[49] D. Maitre, [hep-ph/0703052].

[50] T. Hurth and G. Isidori, private communication.

[51] A. H. Hoang, A. Jain, I. Scimemi and I. W. Stewart, [arXiv:0803.4214].

[52] C. Greub, T. Hurth and D. Wyler, Phys. Rev. **D54**, 3350 (1996), [hep-ph/9603404].